

## Drug pH-Sensitive Release *in Vitro* and Targeting Ability of Polyamidoamine Dendrimer Complexes for Tumor Cells

Dan LIU, Haiyang HU, Jie ZHANG, Xiuli ZHAO, Xing TANG, and Dawei CHEN\*

School of Pharmacy, Shenyang Pharmaceutical University; 103 Wenhua Road, Shenyang, Liaoning Province, 110016, P. R. China. Received July 28, 2010; accepted October 1, 2010; published online October 22, 2010

Recently, dendrimers have been widely used in medical applications such as drug delivery and gene transfection. In this study, a pH-sensitive diblock copolymer of poly(methacryloyl sulfadimethoxine) (PSD) and polyethylene glycol (PEG) modified by lactose (LA-PEG-*b*-PSD) was synthesized. The  $pK_a$  value of the LA-PEG-*b*-PSD was also measured. Then, polyamidoamine (PAMAM) complexes were prepared with PAMAM (G4.0) and LA-PEG-*b*-PSD by electrostatic interaction. To investigate drug pH-sensitive release *in vitro*, doxorubicin (DOX) was loaded in PAMAM. A higher drug cumulative release from LA-PEG-*b*-PSD/PAMAM complexes in phosphate buffered saline (PBS) was found at pH 6.5 than at pH 7.4. The cytotoxicity and cellular uptake of PAMAM complexes were investigated by 3-(4,5-dimethylthiazol-2-yl)-2,5-diphenyltetrazolium bromide (MTT) assay and confocal microscopy. LA-PEG-*b*-PSD/PAMAM/DOX complexes were able to enhance the cytotoxicity of DOX against HepG2 cells at pH 7.4. Confocal microscopy showed a higher cellular uptake of PEG-*b*-PSD/PAMAM complexes at pH 6.5. PAMAM complexes modified by lactose showed a higher affinity for hepatic cancer cells than those without lactose at pH 7.4. These results suggest that LA-PEG-*b*-PSD/PAMAM complexes exhibit selective targeting and cytotoxicity against HepG2 cells. *In vivo* antitumor studies showed that the LA-PEG-*b*-PSD/PAMAM/DOX complexes displayed higher antitumor efficacy compared with non-targeted PAMAM/DOX and DOX solution. These results indicate that this strategy should be applicable to the treatment of liver cancers.

**Key words** polyamidoamine dendrimer; complex; doxorubicin; pH-sensitivity; cytotoxicity; antitumor efficacy

In cancer therapy, several methods have been used to target tumors, and many novel drug carriers are also used to deliver cytotoxic drugs to a particular cell type or tissue in a site-specific manner. It could be beneficial in cancer therapy if cytotoxic drugs can kill tumor cells while not producing their toxic side effects in healthy tissue. In recent years, polyamidoamine (PAMAM) dendrimers have been investigated as carriers for gene delivery, magnetic resonance, the development of vaccines, antivirals, antibacterials and anticancer therapies.<sup>1–5</sup> The advantage of PAMAM dendrimers as a drug carrier is that they are highly branched macromolecules, small in size with a low polydispersity.<sup>6</sup>

Ideal PAMAM dendrimers used as a drug delivery system should be non-toxic, non-immunogenic and biodegradable. However, as observed with other cationic macromolecules, including liposomes and polymeric micelles, PAMAM dendrimers with positively charged surface groups are prone to destabilize cell membranes and cause cell lysis. One way to reduce the cytotoxicity of cationic dendrimers involves partial surface derivatization with chemically inert functionalities such as polyethylene glycol (PEG)<sup>7</sup> or fatty acids. The cytotoxicity of PAMAM dendrimers towards A549 human lung epithelial carcinoma cells can be reduced significantly after modification with hydroxyl groups and PEG.<sup>8,9</sup> This observation can be explained by the reduced overall positive charge on these surface-modified dendrimers. PAMAM dendrimers (G4.0) enter A549 human lung epithelial carcinoma cells more rapidly than those modified with hydroxyl groups and PEG. The cationic nature of the amine surface groups may lead to interaction with negatively charged epithelial cells and allow cell entry *via* fluid phase pinocytosis. The cellular entry of OH-PAMAM and PEG-PAMAM may result from non-specific adsorption to the cell membrane and subsequent endocytosis, and the specific interactions with tumor cells also can be prevented.

It is well documented in literature that the extracellular pH value of tumors is lower than that of normal tissues, for example, a pH of below 7.0 in tumors and 7.4 in normal tissues.<sup>10</sup> The use of a pH-sensitive cleavable linkage between PEG and PAMAM dendrimers may be one feasible approach to deliver drugs to desired tissue sites with low cytotoxicity in normal tissue cells and a long circulation time in blood. Xu *et al.*<sup>11</sup> have synthesized one pH-sensitive PEG conjugated lipid *via* esterase-catalyzed PEGylation linkages. The results obtained suggested that vesicles modified by PEG with ester linkages allowed not only stabilization of the vesicles and prolongation of the circulation time in blood, but also removal of the PEG chain at suitable sites.

Sulfadimethoxine (SD) and polysulfadimethoxine (PSD)<sup>12,13</sup> are widely used to prepare pH-sensitive drug carriers. Sulfonamides and polysulfadimethoxine are weakly acidic due to the readily ionizable hydrogen atom in the amide bond in water. Above the  $pK_a$ , SD and PSD have a negative charge, while they are neutral below the  $pK_a$ . A suitable degree of polymerization and  $pK_a$  have been selected to examine the response to the pH of tumor tissues.<sup>14</sup>

Indeed, the attachment of a cell-specific ligand to PAMAM dendrimers is reported to be a promising way to achieve a higher drug accumulation in tumor cells.<sup>15</sup> It has been found that asialoglycoprotein (ASGP) receptors were widely expressed on the surface of hepatoma cells.<sup>16,17</sup> The terminal  $\beta$ -D-galactose or *N*-acetylgalactosamine residues can be recognized by ASGP receptors and they are widely used in drug carriers as specifically targeting ligands.<sup>18</sup> Many reports suggest that lactose-conjugated PAMAM dendrimers may facilitate binding to ASGP receptors and subsequent uptake into hepatic cells.<sup>19–23</sup>

In the present research, lactose-poly(ethylene glycol)-poly(methacryloyl sulfadimethoxine) diblock copolymer (LA-PEG-*b*-PSD) and poly(ethylene glycol)-poly(methacry-

\* To whom correspondence should be addressed. e-mail: chendawei@syphu.edu.cn

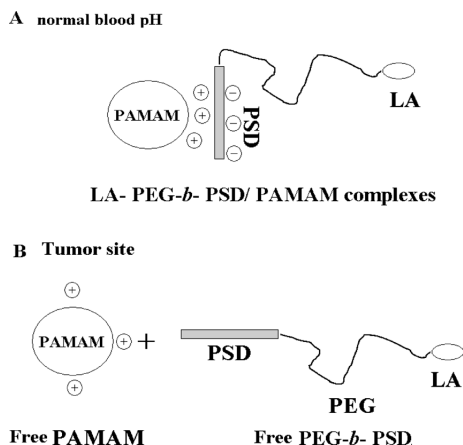


Fig. 1. Schematic Model for the Proposed Drug Delivery System: The Carrier System Consists of Two Components, a PAMAM and a pH-Sensitive Diblock Polymer LA-PEG-*b*-PSD

(A) At normal blood pH, the sulfonamide is negatively charged, and when mixed PAMAM, shields PAMAM by electrostatic interaction; (B) when the system experiences a decrease in pH (at tumor site) sulfonamide loses charge and detaches, thus exposing PAMAM for interaction with tumor cells.

loyl sulfadimethoxine) diblock copolymer (PEG-*b*-PSD) were synthesized. The pH-sensitive PAMAM complexes modified with lactose were prepared with PAMAM dendrimers and LA-PEG-*b*-PSD. Schematic model for the proposed drug delivery system was shown in Fig. 1. To investigate drug pH sensitive release, doxorubicin (DOX) was encapsulated in PAMAM dendrimers. The physicochemical properties of the complexes were studied and their ability to target HepG2 cells was investigated by 3-(4,5-dimethylthiazol-2-yl)-2,5-diphenyltetrazolium bromide (MTT) assay and confocal microscopy. Finally, the antitumor efficacy *in vivo* was studied in tumor-bearing mice.

## Experimental

**Materials** Sulfadimethoxine [4-amino-*N*-(2,6-dimethoxy-4-pyrimidinyl)benzenesulfonamide] (SD), methacryloyl chloride, *o*-(2-aminoethyl)-*o*-(2-carboxyethyl)-polyethylene glycol<sub>3000</sub> hydrochloride (NH<sub>2</sub>-PEG<sub>3000</sub>-COOH), 2,2'-azobis(isobutyronitrile) (AIBN), mercaptoethylamine, *N*-hydroxysuccinimide (NHS), and *N,N'*-dicyclohexylcarbodiimide (DCC) were purchased from Sigma Chemical Co., Ltd. (St. Louis, MO, U.S.A.); lactobionic acid calcium salt was purchased from Fluka Chemical Co., Ltd. (Buchs, Switzerland); PAMAM dendrimers (G4.0, with-NH<sub>2</sub> end groups, ethylenediamine core) were purchased from Sigma Chemical Co., Ltd. (St. Louis, MO, U.S.A.); doxorubicin hydrochloride (DOX·HCl) was purchased from Beijing Huafeng United Technology Co., Ltd. (Beijing, China), RPMI 1640, penicillin-streptomycin (PS, 10000 U/ml) and trypsin-ethylenediaminetetraacetic acid (EDTA) (TE, 0.5% trypsin, 5.3 mM EDTA tetrasodium) were obtained from Gibco BRL (Gaithersburg, MD, U.S.A.); fetal bovine serum (FBS) was purchased from Sijiqing Biologic Co., Ltd. (Hangzhou, China). AIBN was recrystallized twice in methanol, *N,N*-dimethylformamide (DMF) was purified by vacuum distillation at 75 °C at 12 mmHg, and all other chemicals were of reagent grade and used without further purification.

**Synthesis of Poly(vinyl sulfadimethoxine) (PSD)** Sulfadimethoxine methacrylamide (SDM) was synthesized as described earlier.<sup>13</sup> Briefly, SD (0.5 g, 1.6 mmol) was dissolved in 20 ml acetone/water (1 : 1, v/v) which contained sodium hydroxide (0.01 N). Methacryloyl chloride (10 mmol) was added dropwise to SD solution at 0 °C with vigorous stirring. After filtration, the SDM precipitate was washed three times with distilled water. A white powder was collected after drying in vacuum at room temperature for 48 h, yielding 85%. The IR spectrum of SDM showed one sharp absorption peak at 3386 cm<sup>-1</sup>, instead of the primary and secondary amine at 3450 cm<sup>-1</sup>, 3348 cm<sup>-1</sup> and 3229 cm<sup>-1</sup> of SD, which confirmed the disappearance of the primary amine. The carbonyl amide absorption peak appeared at 1676 cm<sup>-1</sup>. The peaks of four protons in the <sup>1</sup>H-NMR spectrum of the benzene ring of

SDM shifted to 7.8 ppm (dd, 7.5, 6.5 ppm in SD).

The semitelechelic polymer was synthesized by free radical solution polymerization. SDM (0.5 g, 1.27 mmol), AIBN (initiator, 0.2 mol% of the monomer, 0.42 mg, and 0.0025 mmol) and mercaptoethylamine (a chain transfer agent, 1.96 mg, and 0.025 mmol) were dissolved in DMF (10 ml) which had been degassed to remove of oxygen by bubbling with N<sub>2</sub> gas for 12 h. The mixture was degassed by the freeze-thaw cycle method and sealed under reduced pressure. After a polymerization reaction in an oil bath at 70 °C for 20 h, the solution was poured into deionized water to precipitate the product. The polymer was collected by filtration, and washed with a 10-folds volume of methanol at room temperature for 24 h to remove the residual SDM. The final product (PSD) was collected by filtration and then dried in vacuum at room temperature. The polymer yield was 70%. In the <sup>1</sup>H-NMR spectrum of PSD, the methylene (-H<sub>2</sub>C=C-) peak of SDM disappeared after polymerization and the benzene peak was shifted down-field to 7.9–8.0 ppm ( $\delta$  7.8 ppm in SDM). <sup>1</sup>H-NMR:  $\delta$  11.6 ppm (-SONH-),  $\delta$  9.6 ppm (-CONH-),  $\delta$  7.9–8.0 ppm (phenylene-H),  $\delta$  6.9 ppm (pyrimidinyl-H),  $\delta$  3.6 ppm (pyrimidinyl -N=C-OCH<sub>3</sub>). The molecular weight was 3 kDa (polydispersity index (PDI)=1.15) determined by GPC (Waters 1515, Waters, U.S.A.).

**Synthesis of Lactose-Poly(ethylene glycol)-Poly(vinyl sulfadimethoxine) Diblock Copolymer (LA-PEG-*b*-PSD)** A solution of lactobionic acid calcium salt was passed through a cation-exchange resin column (Dowex 50WX8) to convert it to free lactobionic acid. The eluted free acid (pH value <3) was collected and lyophilized to give a powder. Lactobionic acid (43 mg, 0.12 mmol), S-NHS (27.6 mg, 0.24 mmol) and 1-(3-dimethylaminopropyl)-3-ethylcarbodiimide (EDC) (46 mg, 0.24 mmol) were dissolved in 20 ml distilled water with stirring for 10 h at room temperature, then NH<sub>2</sub>-PEG<sub>3000</sub>-COOH (300 mg, 0.1 mmol) was added with stirring for 12 h. The mixture was then dialyzed (molecular weight cutoff (MWCO): 1 kDa) against water for 48 h and the product (COOH-PEG<sub>3000</sub>-LA) was dried in vacuum at room temperature. The IR spectrum showed absorption peaks at 1646 cm<sup>-1</sup> (amide,  $\nu$ C=O) and 1613 cm<sup>-1</sup> (amide,  $\beta$ -NH), which indicated the appearance of a secondary amide. <sup>1</sup>H-NMR spectrum (DMSO):  $\delta$  10.7 (H, -COOH),  $\delta$  5.20 ppm (H, -CONH-),  $\delta$  4.0–4.3 ppm (-H, lactobionic residue), and  $\delta$  3.4–3.6 ppm (H, (-CH<sub>2</sub>-CH<sub>2</sub>-O)<sub>n</sub>).

LA-PEG-COOH was activated in 10 ml dimethyl sulfoxide (DMSO) by S-NHS (PEG : NHS : DCC = 1 : 2 : 2, m/m) for 10 h, then PSD (PEG : PSD = 1 : 1.5, m/m) was added to the mixture followed by stirring overnight at room temperature. The product (LA-PEG-PSD) was purified by dialyzing (MWCO: 5.0 kDa) for 48 h. The polymer yield was 75%. The chemical structure was confirmed by the <sup>1</sup>H-NMR spectrum:  $\delta$  10.83 ppm (1H, s, -SO<sub>2</sub>NH-pyrimidinyl),  $\delta$  8.14–8.27 ppm (4H, dd, phenylene-H), and  $\delta$  3.83–3.76 ppm (6H, m, pyrimidinyl -N=C-OCH<sub>3</sub>),  $\delta$  3.4–3.6 ppm (H, (-CH<sub>2</sub>-CH<sub>2</sub>-O)<sub>n</sub>), and  $\delta$  3.8–4.1 ppm (-H, lactobionic residue). <sup>13</sup>C-NMR (DMSO): ( $\delta$  172.402 ppm, c), ( $\delta$  171.983 ppm, h), ( $\delta$  167.566 ppm, m), ( $\delta$  164.722 ppm, e), ( $\delta$  160.879 ppm, k), ( $\delta$  157.43 ppm, l), ( $\delta$  128.1 ppm, j), ( $\delta$  119.762 ppm, i), ( $\delta$  106 ppm, a) ( $\delta$  85.094 ppm, b), ( $\delta$  69 ppm, d), ( $\delta$  53.866 ppm, n), ( $\delta$  40.078 ppm, f), ( $\delta$  24.48 ppm, g). The mean molecular weight was 6.0 kDa (PDI=1.49) determined by GPC. Synthesis schemes of LA-PEG-*b*-PSD were shown in Fig. 2. PEG-*b*-PSD was synthesized by the same method with PEG-COOH and PSD.

**Synthesis of PEGylated PAMAM (PEG-PAMAM)** The PEGylated PAMAM was obtained after activation of the end functional groups of mPEG-3000. PAMAM G4.0 was dissolved in borate buffer (pH 9.8) and stirred vigorously with PEG-NHS (molecular weight (Mw): 3000) (PAMAM G4.0 : PEG-NHS = 1 : 13, m/m) overnight at room temperature in the dark. The final product was dialyzed to remove byproducts (MWCO: 5.0 kDa), and the dialyzed product was then concentrated and lyophilized. The major change of mPEG-COOH in IR spectrum was carbonyl resonating symmetric and anti-symmetric peaks on linking *via* the amide at the dendrimeric ends. An important IR peak near 1112 cm<sup>-1</sup> of the ether linkage C-O was clearly present in the spectrum of the PEGylated dendrimers 4.0G. <sup>1</sup>H-NMR:  $\delta$  2.2–3.0 ppm (-CH<sub>2</sub>-, PAMAM),  $\delta$  3.22 ppm (-OCH<sub>3</sub>-, PEG),  $\delta$  3.45–3.80 ppm (-CH<sub>2</sub>O-, mPEG).

**The pK<sub>a</sub> Determination of LA-PEG-*b*-PSD** The pK<sub>a</sub> values of SD, PSD, PEG-*b*-PSD and LA-PEG-*b*-PSD were measured by potentiometric titration (auto potentiometric titrimer ZDJ-4A1.0, Shanghai Leici Co., Ltd., Shanghai, China). LA-PEG-*b*-PSD (SD, PSD and PEG-*b*-PSD) was dissolved in 0.01 N standard NaOH solution, and the volumetric solution was 0.01 N HCl. The electric potential of the solution after each HCl addition was measured. All the measurements were performed at 25 °C.

**Loading DOX into PAMAM Dendrimers** The HCl salt in DOX·HCl was removed by triethylamine. Briefly, DOX·HCl was dissolved in 30 ml

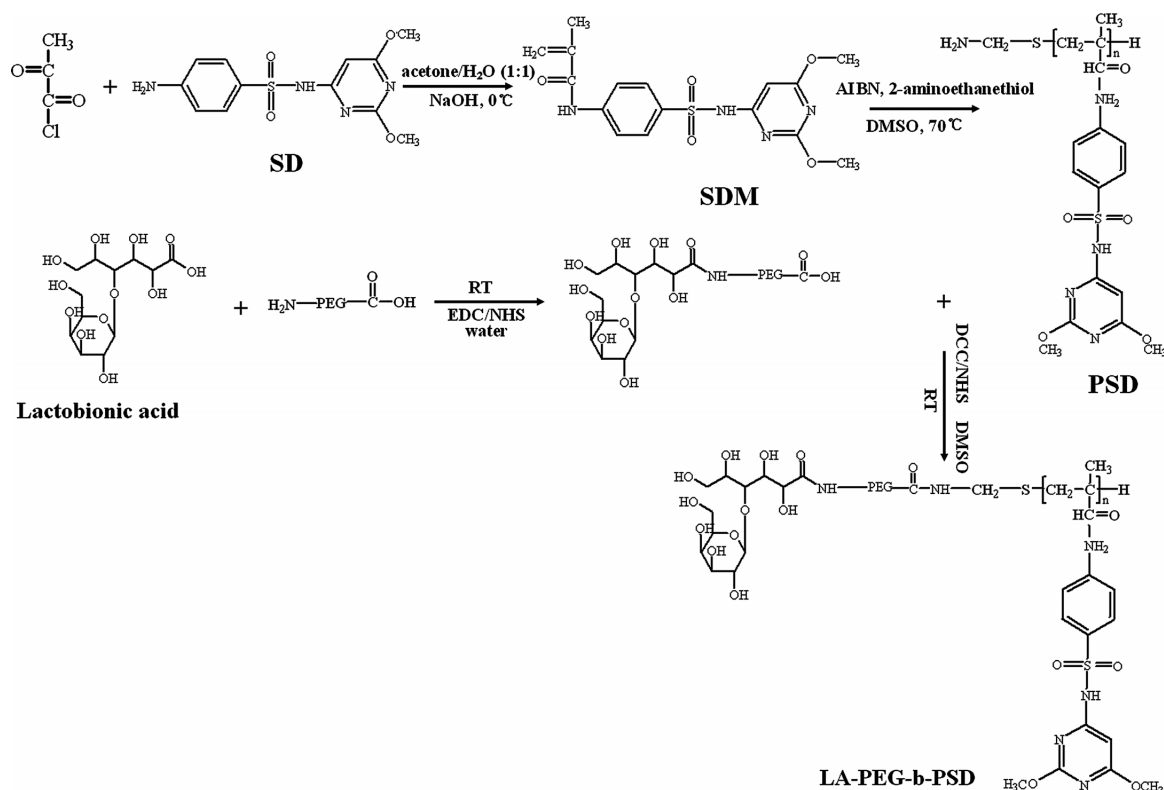


Fig. 2. Synthesis Schemes of LA-PEG-*b*-PSD

methanol/acetone (1:1, v/v), and then triethylammonium acetate (TEA) (3.0-fold excess of DOX·HCl) was added with stirring in the dark for 24 h. After filtration, the solvent was removed by rotary evaporation in a vacuum. The DOX precipitate was washed three times with distilled water to remove residual DOX·HCl and TEA. After filtering, DOX was dried in a vacuum at room temperature for 48 h.

DOX and PAMAM dendrimers (PEG-PAMAM dendrimers) were dissolved in 30 ml methanol with in a molar ratio of 3:1. The mixture was stirred in the dark at room temperature for 24 h, and then methanol was removed completely by rotary evaporation in a vacuum. Then, 10 ml phosphate buffer (pH 7.4) was added with stirring for 24 h to dissolve the PAMAM dendrimers. After filtration, the free doxorubicin was separated from DOX/PAMAM dendrimers with a Sephadex G50 column before LA-PEG-PSD/DOX/PAMAM complexes were prepared. the DOX incorporation efficiency (%) was calculated by the formula: the drug entrapment efficiency (%) = the amount of DOX in PAMAM dendrimers / (the amount of free DOX + the amount of DOX in PAMAM dendrimers).

**Preparation of LA-PEG-*b*-PSD/PAMAM Complexes** LA-PEG-*b*-PSD/PAMAM complexes were prepared with PAMAM dendrimers and LA-PEG-*b*-PSD. In a typical procedure, LA-PEG-*b*-PSD or PEG-*b*-PSD was dissolved in Na<sub>2</sub>HPO<sub>4</sub> (10 mM, 13.95 ml) and added to a solution of PAMAM in NaH<sub>2</sub>PO<sub>4</sub> (10 mM, 6.05 ml) to give a solution of PAMAM complexes. The ratio of the positive to negative charge was fixed at 1:1. After mixing the two solutions, the pH of the solution was 7.4 (10 mM phosphate buffered saline (PBS)).

**The Effect of pH on the LA-PEG-*b*-PSD/PAMAM Complexes** The effect of different pH values on the changes in particle size was investigated by dynamic laser light scattering. The LA-PEG-*b*-PSD/PAMAM complexes were prepared in phosphate buffer at pH 8.0. The pH value was reduced from 8.0 to 6.0 by adding 0.01 N HCl followed by incubation for 4 h. The particle sizes at different pH values were measured with a Nicomp 380ZLS particle sizer.

**In Vitro Release of Doxorubicin from PAMAM Complexes** *In vitro* release studies were performed using the dialysis bag method. The dialysis bag (molecular weight cut off 8000–14000) was soaked in distilled water for 12 h before use. PAMAM dendrimers, PEG-PAMAM dendrimers, PEG-*b*-PSD/PAMAM complexes and LA-PEG-*b*-PSD/PAMAM complexes were prepared with a DOX concentration of 0.4 mg/ml. Then, 3 ml of the LA-PEG-*b*-PSD/PAMAM complexes or other samples was placed in the dialysis bag and the receptor compartment was filled with 100 ml phosphate buffer

(pH 6.5 or pH 7.4) at 37 °C with gentle agitation (25 rpm). Then, 1.0 ml of the dissolution medium was withdrawn from the receptor compartment at intervals of 1, 2, 3, 4, 5, 7, 10, 12, 24, 48 h and replace with the same volume of fresh dialysis medium. Three milliliters DOX solution (40 μg/ml) was also placed in the dialysis bag to estimate the influence of DOX permeation through the dialysis bag, the receptor compartment was 50 ml, 0.5 ml of the medium was withdrawn at 0.5, 1, 1.5, 2, 2.5, 3, 3.5, 4 h. The DOX content of samples was analyzed by HPLC. The drug release study of PAMAM complexes in blood was performed by adding 2 ml 100% plasma and 1 ml PAMAM complexes to the dialysis bag. The release medium was 100 ml phosphate buffer (pH 7.4), the release medium of DOX solution group was 30 ml phosphate buffer (pH 7.4). All analyses were performed in triplicate to allow statistical analysis.

**Cell Culture** Human hepatic carcinoma (HepG2) cells were used for cell uptake and cytotoxicity studies. Cells were grown in RPMI-1640 medium with 1% penicillin–streptomycin and 10% fetal bovine serum in a humidified incubator at 37 °C and 5% CO<sub>2</sub>. The cells were subcultured every 48 h and harvested from subconfluent cultures (60–70%) using 0.25% trypsin.

**Anticancer Activity *in Vitro*** The cytotoxicity of LA-PEG-*b*-PSD/PAMAM complexes, PAMAM dendrimers, and PEG-*b*-PSD/PAMAM complexes was investigated against Human hepatic carcinoma (HepG2) cells by MTT assay. The cells (5 × 10<sup>7</sup> cells/ml) grown as a monolayer were harvested using 0.25% (w/v) trypsin and seeded in 96-well plates at a density of 7000 cells per well and incubated for 24 h. Then, 300 μl RPMI-1640 medium containing the test samples was added. The PAMAM concentration was 1.0, 5.0, 10.0, 50.0, 100.0, 200 μg/ml, respectively. After 48 h incubation, the cells were washed with PBS, followed by the addition of 20 μl MTT (2 mg/ml), and the cells were then incubated for another 4 h. After incubation, 200 μl DMSO was added to dissolve the crystals. The plates were read immediately on a plate reader at a test wavelength of 570 nm.

The cytotoxicity of LA-PEG-*b*-PSD/PAMAM/DOX complexes, PAMAM/DOX, and PEG-*b*-PSD/PAMAM/DOX complexes was also investigated against Human hepatic carcinoma (HepG2) cells by MTT assay. One hour before the addition of PAMAM complexes, 300 μl RPMI-1640 medium at pH 6.5 or 7.4 was added. Then, 20 μl of PAMAM complexes was added and incubated for 6 h, 24 h and 48 h. The DOX concentration was 10.0 μg/ml, and the PAMAM concentration was 100 μg/ml. After incubation, 20 μl MTT (2 mg/ml) was added and cells were incubated for another 4 h. Then, 200 μl DMSO was added to dissolve the crystals and the plates were read immedi-

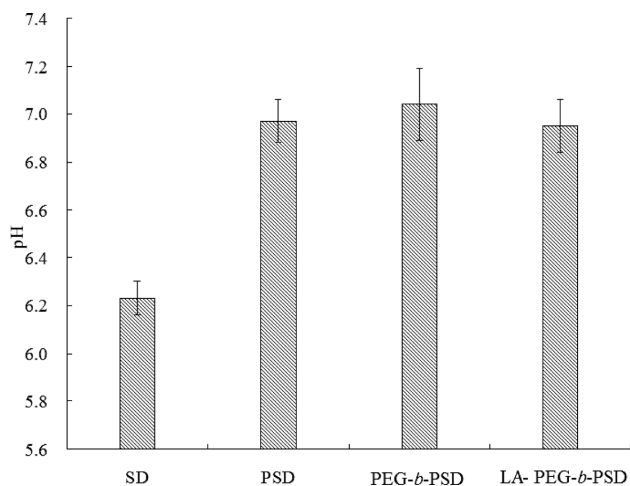


Fig. 3.  $pK_a$  of SD Monomer and Polymerized Derivatives

ately on a plate reader at a test wavelength of 570 nm.

**Confocal Microscopy** PAMAM dendrimers were labeled with fluorescein iso thiocyanate (FITC) before use. FITC (10 mg) was dissolved in 0.5 ml acetone, and then this acetone solution was added to the PAMAM solution (8 mg/ml, pH 8.0). The molar ratio of FITC to  $-NH_2$  on the surface of PAMAM dendrimers was 1 : 10. The reaction mixture was stirred for 24 h at room temperature and dialyzed to remove free FITC. All steps were performed in the absence of light. HepG2 cells were seeded at a density of  $2 \times 10^5$  cells/well on the surface of a cover slide in 6-well plates. Two types of experiment were performed: Type 1) internalization of PEG-*b*-PSD/PAMAM complexes into HepG2 cells at pH 6.5 or pH 7.4. Cells were incubated with PAMAM complexes (the concentration of PAMAM dendrimers was 50  $\mu$ g/ml) for 30 min at pH 6.5 or pH 7.4, and washed with PBS. The cells were observed by confocal laser scanning microscopy (Olympus FV1000-IX81, Tokyo, Japan). Type 2) internalization of LA-PEG-*b*-PSD/PAMAM/DOX complexes and PEG-*b*-PSD/PAMAM/DOX complexes into HepG2 cells at pH 7.4. Cells were incubated with PAMAM complexes with a DOX concentration of 5  $\mu$ g/ml for 4 h at pH 7.4 and washed with PBS, then mounted on a cover slip. The cells were observed by confocal laser scanning microscopy.

**In Vivo Therapeutic Studies** Sixty tumor-bearing mice (25–27 g) were prepared by inoculating a suspension of  $H_{22}$  cells (200  $\mu$ l,  $5 \times 10^7$ ) subcutaneously (s.c.) into each axillary fossa of KM mice. When the tumor diameters had reached 0.5 cm, the mice were divided into six groups each of ten mice. The groups were treated with physiological saline, DOX·HCL solution, PAMAM/DOX; PAMAM-PEG/DOX, PEG-*b*-PSD/PAMAM/DOX complexes and LA-PEG-*b*-PSD/PAMAM/DOX complexes respectively, 5 times at intervals of 1 d. Treatments were given intravenously (i.v.) at a dose of 2 mg DOX/kg mouse weight. On the 12th day after treatment, the mice were sacrificed and the local tumors were removed carefully. The net weights of the tumors were measured.

**Statistical Analysis** All the experiments were repeated at least three times. Statistical comparisons were performed with SPSS 12.0 software. Data are presented as mean values with the standard deviation (mean  $\pm$  S.D.), and  $p \leq 0.05$  was considered to be indicative of statistical significance.

## Results and Discussion

**$pK_a$  of LA-PEG-*b*-PSD** The apparent  $pK_a$  values of SD, PSD, PEG-*b*-PSD and LA-PEG-*b*-PSD were investigated by potentiometric titration. As shown in Fig. 3, the  $pK_a$  of SD was 6.2, and the subacidity of the sulfonamide group was due to the ionization of the N–H bond, the electrons of which were removed by the oxygen atoms of the sulfonyl group from the sulfur atom. It has been confirmed that the  $pK_a$  of ionizable groups usually shifts towards a higher pH value after polymerization.<sup>13,14</sup> In this study, the  $pK_a$  of PSD, PEG-*b*-PSD and LA-PEG-*b*-PSD was about 6.97, 7.04 and 6.95, respectively, which is close to the acidic conditions at the

tumor sites.

**Characterization of LA-PEG-*b*-PSD/PAMAM Complexes** The LA-PEG-*b*-PSD/PAMAM complexes were prepared with LA-PEG-*b*-PSD carrying a negative charge and PAMAM dendrimers carrying a positive charge. An almost 94% incorporation of DOX into the PAMAM dendrimer was achieved at a DOX to PAMAM molar ratio of 3 : 1. As the charge ratio of positive charge to negative charge decreased, the  $\zeta$  potential gradually also decreased (data not shown). The  $\zeta$  potential was around 0 mV at a charge ratio of 1 : 1, which indicated that all the positive charge of PAMAM was interact with the negative charge of the LA-PEG-*b*-PSD. In general, less particle aggregation occurred at high zeta potential due to electric repulsion.<sup>24</sup> The sterically repulsive character of the PEG layer prevented the complexes from undergoing secondary aggregation, and their high dispersivity remained high in aqueous medium.

The size of the PAMAM (G4.0) dendrimers was about 4 nm.<sup>25</sup> In this study, the particle size was measured by dynamic light scattering. As the charge ratio (+/–) increased from 1 : 1 to 5 : 1, the particle size of the PAMAM complexes decreased. The average particle size was 54 nm (1 : 1, +/–) and 50 nm (2 : 1, +/–), respectively. When the charge ratio was higher than 3 : 1, the size was less than 20 nm. According to particle size and  $\zeta$  potential, the complexes were prepared at charge ratio (1 : 1, +/–). The enhanced permeability and retention (EPR) effect in tumors is important for the delivery of nanocarriers from blood vessels to tumors, and this is affected by the particles size. In this study, at a charge ratio (+/–) of 1 : 1, the particle size (54 nm) of LA-PEG-*b*-PSD/PAMAM complexes was suitable for penetration of blood vessel with EPR effect.

The morphology of LA-PEG-*b*-PSD/PAMAM complexes at charge ratio (1 : 1, +/–) was observed using transmission electron microscope (TEM) (Fig. 4). LA-PEG-*b*-PSD/PAMAM complexes existed in the form of spherical particles of about 50 nm which was consistent with the result of dynamic light scattering.

**The Effect of pH on LA-PEG-*b*-PSD/PAMAM Complexes** The effect of different pH values on the changes in particle size was investigated to test the shielding/deshielding of the pH-sensitive polymer. As shown in Fig. 5, no significant difference in the average particle size was found between pH 8.0 and 7.0 (above 50 nm). When the pH was less than 7.0, the particle size fell slightly. At pH 6.8, the particle size of LA-PEG-*b*-PSD/PAMAM complexes was 34 nm, and this might be due to the incomplete complexation of LA-PEG-*b*-PSD and PAMAM. From pH 6.6 to 6.0, there was no significant difference in the average particle size (less than 10 nm).

**The Influence of pH on Drug Release** To evaluate a pH-sensitive drug carrier, the drug release *in vitro* is an important parameter. As shown in Figs. 6 and 7, the drug release of PAMAM dendrimers, PEG-PAMAM dendrimers and PAMAM complexes was studied in PBS at pH 7.4 and pH 6.5. The cumulative release of DOX from LA-PEG-*b*-PSD/PAMAM complexes and PEG-*b*-PSD/PAMAM complexes at 48 h (pH 7.4) was about 40%. However, the release rate of DOX from PAMAM dendrimers was faster, being over 80% at 48 h. These results indicated that the complexes could reduce the drug release rate at a physiological pH



Fig. 4. TEM of the LA-PSD-*b*-PEG/PAMAM Complexes Micelles ( $\times 100000$ ), Bar: 100 nm

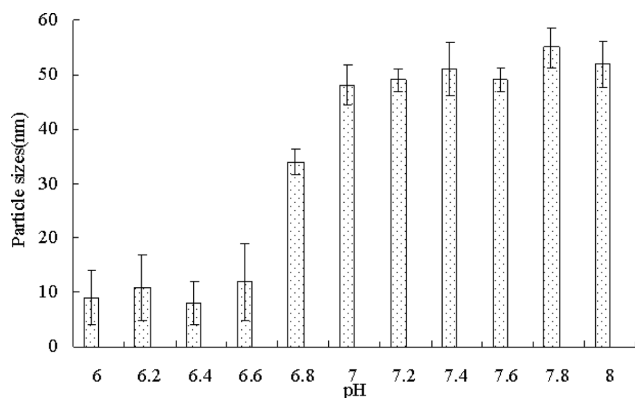


Fig. 5. Particle Sizes of LA-PEG-*b*-PSD/PAMAM Complexes at Different pH Values ( $n=3$ )

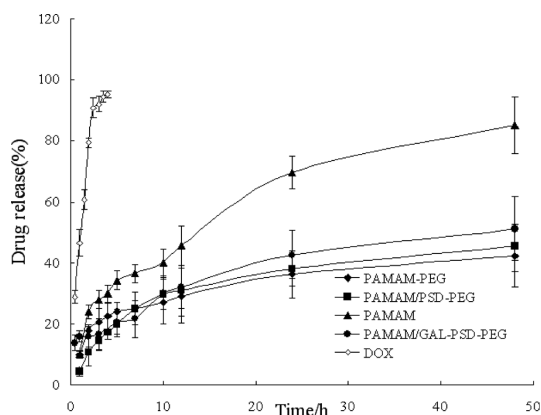


Fig. 6. The Release of Doxorubicin from PAMAM Complexes in PBS (pH 7.4) ( $n=3$ )

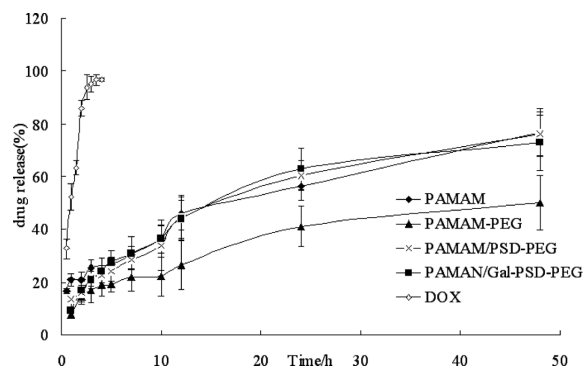


Fig. 7. The Release of Doxorubicin from PAMAM Complexes in PBS (pH 6.5) ( $n=3$ )

value. And these should be contribute to 1) more sealing of dendrimeric structure by PEG at the peripheral portions of dendrimers as coat, which prevented drug release by enhancing complexation probably by steric effect; 2) reducing the amount of positive charge on the surface of PAMAM dendrimers by modified with PEG or PEG-PSD, which can increase the hydrophobic of PAMAM dendrimers. Compared with the PEG-PAMAM with a covalent linkage, the PEG on the complexes had a similar shielding effect. The drug release at pH 6.5 (Fig. 7) was different, with the cumulative release of DOX from PAMAM complexes and PAMAM dendrimers being over 70% in every case, and higher than that of PEG-PAMAM dendrimers. The electrostatic force between LA-PEG-*b*-PSD (PEG-*b*-PSD) and PAMAM dendrimers was abolished at pH 6.5 and the complexes disintegrated into free PAMAM dendrimers. Also this could be confirmed by the results shown in Fig. 5. The same release behavior of the LA-PEG-*b*-PSD/PAMAM complexes and PEG-*b*-PSD/PAMAM complexes at pH 6.5 and pH 7.4 showed that the shielding effect of PEG was not affected by the lactose residue conjugated to the end of PEG-*b*-PSD. The cumulative release of DOX solution was nearly 98% within 4 h in both buffers, it indicated that the release of DOX could not be affected by dialysis bag.

Full generation of PAMAM dendrimers had primary amine end groups ( $-NH_2$ ) on the surface and tertiary amine groups ( $NH^-$ ) at the branching points in the core, having  $pK_a$  values of 9–10 ( $pK_{a1}$ ) and 2–4 ( $pK_{a2}$ ).<sup>26–28</sup> At pH 7.4 and pH 6.5, the hydrophobic interactions between PAMAM and DOX were favorable. The DOX was encapsulated in PAMAM by a hydrophobic interaction, and the drug release behavior depended on hydrophobic diffusion, so the release behavior of PAMAM/DOX at pH 7.4 and 6.5 showed a similar trend. An earlier experiment demonstrated the drug release behavior of PAMAM dendrimer–drug conjugates with different linkers.<sup>29</sup> Their results confirmed that the amide bonds are too stable for hydrolysis, and the drug release was quite slow up to pH 1.2.

**DOX Release from LA-PEG-*b*-PSD/PAMAM Complexes in Plasma** Plasma contains many types of ions and plasma protein, which can interact with PAMAM complexes and reduced the electrostatic interaction between PAMAM and the diblock copolymer. Drug release in plasma was necessary to investigate the stability of PAMAM complexes *in vivo*. In this study, rat plasma was used. The cumulative release of DOX from the LA-PEG-*b*-PSD/PAMAM complexes

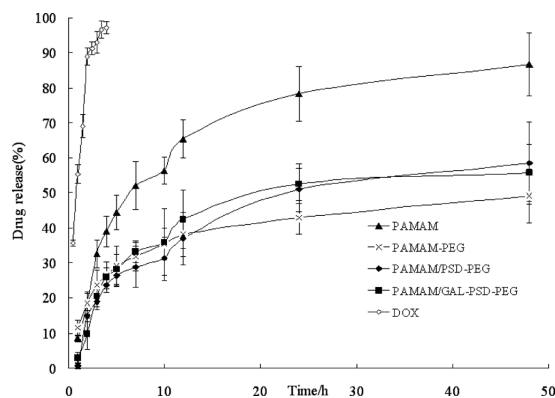


Fig. 8. The Release of Doxorubicin from PAMAM Complexes in Plasma ( $n=3$ )

Table 1. Viability of HepG2 Cells in the Presence of Blank PAMAM, PEG-*b*-PSD/PAMAM Complexes, and LA-PEG-*b*-PSD/PAMAM Complexes in the Medium ( $n=6$ )

Concentration ( $\mu\text{g/ml}$ )	PAMAM	% cells viability PEG- <i>b</i> -PSD/PAMAM complexes	LA-PEG- <i>b</i> -PSD/PAMAM complexes
1	99.23 $\pm$ 1.2	101.2 $\pm$ 1.5	99.2 $\pm$ 3.8
5	98.7 $\pm$ 2.9	99.1 $\pm$ 2.4	99.3 $\pm$ 2.6
10	97.8 $\pm$ 2.0	98.7 $\pm$ 3.6	99.9 $\pm$ 2.2
50	97.4 $\pm$ 3.8	97.4 $\pm$ 2.7	97.3 $\pm$ 3.9
100	95.5 $\pm$ 3.6	96.2 $\pm$ 4.2	96.1 $\pm$ 2.8
200	94.77 $\pm$ 4.2	96.05 $\pm$ 3.7	96.89 $\pm$ 2.1

and PEG-*b*-PSD/PAMAM complexes was higher than that of PAMAM-PEG (Fig. 8). This indicated that PAMAM complexes were resistant in plasma. However, the complexes were not as stable as PAMAM-PEG in plasma, perhaps because the electrostatic interaction between PAMAM and PEG-*b*-PSD could be destroyed to some degree by plasma proteins and ions. Compared with PAMAM, the release of DOX from the PEG-PAMAM, LA-PEG-*b*-PSD/PAMAM complexes and PEG-*b*-PSD/PAMAM complexes was slower.

Although particle carriers modified by non-cleavable PEG were stable and potentially had a long circulation time *in vivo*, they could not release their content at the desired site faster and could not be taken up by cells quickly due to the non-removable PEG-coatings. Compared with the PAMAM-PEG, the LA-PEG-*b*-PSD/PAMAM (PEG-*b*-PSD/PAMAM) complexes had a cleavable PEG barrier at a site *in vivo*. The complexes could disintegrate at the target region. Furthermore, the PAMAM could be taken up easily by the tumor cells and release the drug rapidly.

**The Anticancer Activity of LA-PSD-*b*-PEG/PAMAM Complexes *in Vitro*** As shown in Table 1, the cytotoxicity of all blank formulations against HepG2 cell was essentially negligible at PAMAM concentration of 100  $\mu\text{g/ml}$ .

It is well known that efficient liver targeting can be achieved by the action of lactose.<sup>30–32</sup> In this study, MTT assay was used to investigate the cytotoxicity against HepG2 cells, which expressed asialoglycoprotein receptors, and the targeting ability of the LA-PEG-*b*-PSD/PAMAM complexes against HepG2 cells was also studied. Cells were incubated with PAMAM or PAMAM complexes for 6 h, 24 h and 48 h at difference pH values.

The growth-inhibiting activity of all the formulations at

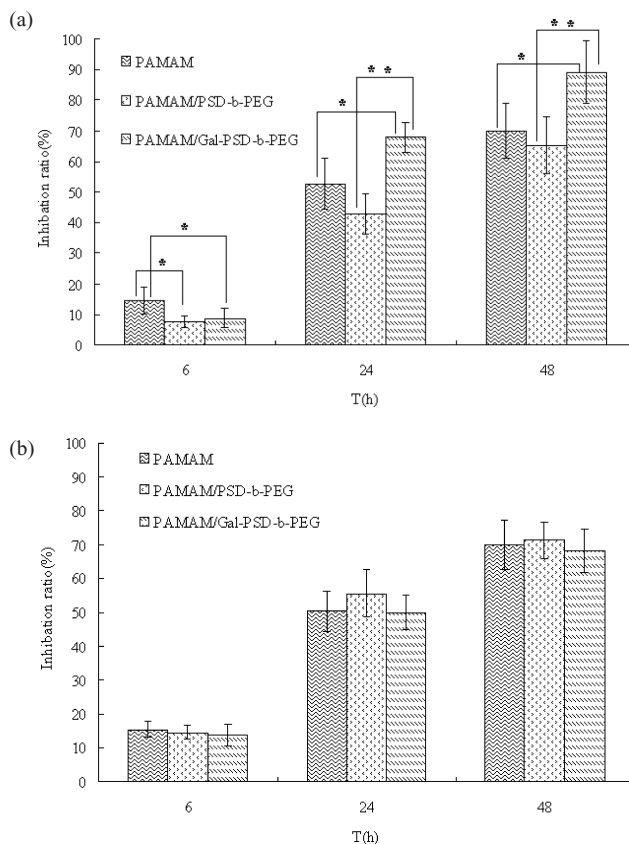


Fig. 9(A). The Cell Cytotoxicity of PAMAM/DOX, PEG-*b*-PSD/PAMAM/DOX Complexes and LA-PEG-*b*-PSD/PAMAM/DOX Complexes on HepG2 Cells, the Cells Were Incubated at pH 7.4 for 6 h, 24 h, and 48 h, Respectively ( $n=6$ )

\*  $p < 0.1$ , \*\*  $p < 0.05$ .

(B). The Cell Cytotoxicity of PAMAM/DOX, PEG-*b*-PSD/PAMAM/DOX Complexes and LA-PEG-*b*-PSD/PAMAM/DOX Complexes on HepG2 Cells, the Cells Were Incubated at pH 6.5 for 6 h, 24 h, and 48 h, Respectively ( $n=6$ )

pH 7.4 was shown in Fig. 9A, and that at pH 6.5 was shown in Fig. 9B. After a 6 h incubation, the growth inhibition ratio of PAMAM/DOX at pH 7.4 ( $14.49 \pm 4.3\%$ ) was higher than that of the PEG-*b*-PSD/PAMAM/DOX complexes ( $7.56 \pm 2.09\%$ ) and the LA-PEG-*b*-PSD/PAMAM/DOX complexes ( $8.74 \pm 3.12\%$ ) (Fig. 9A) ( $p \leq 0.05$ ). This should contribute to the cationic nature of the dendrimers, which interact with the negative charge on the cell surface. Besides tumor cells, this interaction could occur on the surface of the cells of other tissues. Compared with PAMAM/DOX, the affinity of the PEG-*b*-PSD/PAMAM/DOX complexes and the LA-PEG-*b*-PSD/PAMAM/DOX complexes for normal tissues was smaller. The internalization of the two PAMAM complexes was restricted by the PEG shell. The growth inhibiting activity of LA-PEG-*b*-PSD/PAMAM/DOX complexes was  $67.76 \pm 4.69\%$  at 24 h and  $89.02 \pm 10.27\%$  at 48 h, which was much higher than that of the PEG-*b*-PSD/PAMAM/DOX complexes ( $42.65 \pm 6.58\%$  at 24 h,  $65.34 \pm 9.23\%$  at 48 h) and PAMAM/DOX ( $52.67 \pm 8.21\%$  at 24 h,  $69.93 \pm 8.98\%$  at 48 h). These results suggested that the attachment of lactose moieties increased the internalization of LA-PEG-*b*-PSD/PAMAM/DOX complexes through the receptor-mediated endocytosis mechanism, and this played a major role in 24 h

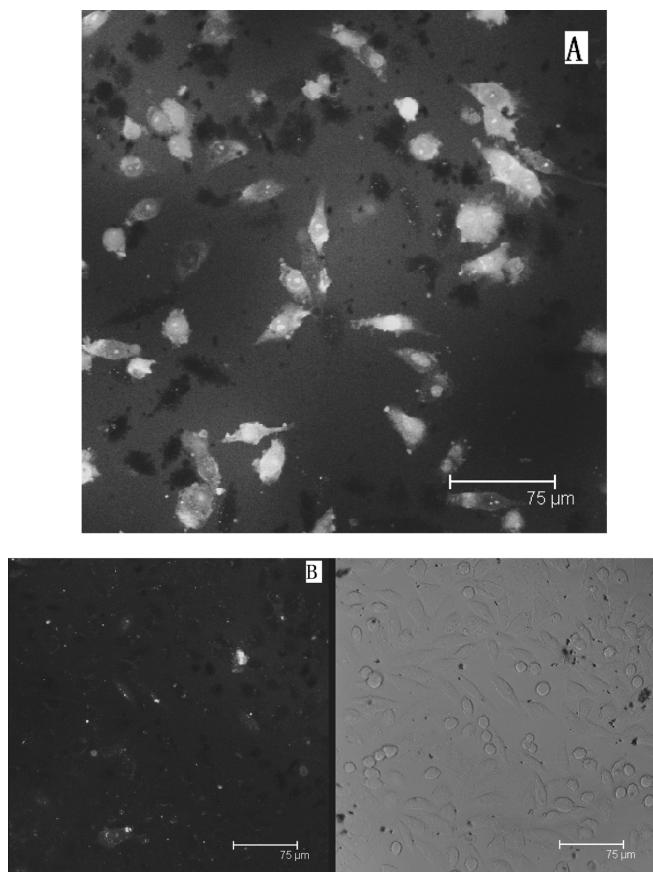


Fig. 10. Confocal Micrographs of HepG2 Cells Incubated for 30 min with PEG-*b*-PSD/PAMAM Complexes at (A) pH 6.5 and (B) pH 7.4

and 48 h incubation.

At pH 6.5, the inhibition ratio of the two complexes was a little lower than PAMAM/DOX at 6 h (Fig. 9B). However, no significant difference in anticancer activity was found in all the formations at 24 h and 48 h. These results were consistent with the drug release *in vitro* at pH 6.5. At pH 6.5, the attachment of PEG and lactose moieties was abolished and this was supported by the results in Fig. 5.

As the results shown in Figs. 9A and 9B, involvement of pH-sensitive moieties and the receptor-mediated pathway markedly enhance the cellular targeting ability.

**Confocal Microscopy. Internalization of PEG-*b*-PSD/PAMAM Complexes at Different pH Values** Confocal laser scanning microscopy was used to investigate the internalization of PAMAM complexes, and the internalization of PAMAM complexes was tested at pH 6.5 and pH 7.4. The results (Figs. 10A, B) were consistent with those of the MTT assay. After a 30 min incubation at pH 6.5, PEG-*b*-PSD/PAMAM complexes were taken up by the cells (Fig. 10A), which indicated that the linkage between PEG and PAMAM was cleaved at pH 6.5. However, the micrographs in Fig. 10B showed different results. Very little of the PEG-*b*-PSD/PAMAM complexes was taken up by the cells. PEG-*b*-PSD/PAMAM complexes were stable at pH 7.4 and the PEG chain could prevent the effective uptake by cells. Those results were also confirmed by the cytotoxicity study. Others<sup>33</sup> have reported similar results showing that TAT micelles conjugated with PEG-poly(methacryloyl sulfadimethoxine) were shielded at normal pH, but deshielded at the pH value of the

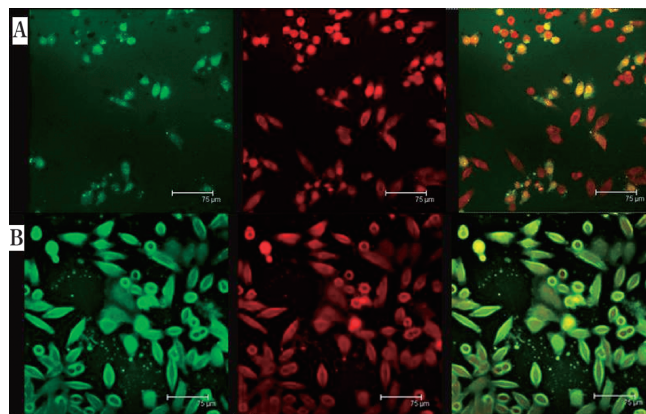


Fig. 11. Dual Label Confocal Micrographs of HepG2 Cells Incubated with (A) PEG-*b*-PSD/PAMAM/DOX Complexes, (B) LA-PEG-*b*-PSD/PAMAM/DOX Complexes

Cells stained with green with FITC attached to PAMAM, red was DOX, and yellow was the superimposed image of the two micrographs.

tumor sites.

Nanoparticle drug carriers are usually not very stable in plasma, resulting in a failure to deliver their contents to their targeted sites. Some studies are reported on modifying nanoparticle drug carriers with PEG to prolong their circulation time in blood. In this study, we wanted the PEG shell to be removed at the tumor site, and not prevent cells endocytosis.<sup>34–36</sup>

Cationic dendrimers exhibited strong electrostatic interactions with cells, and rapidly became endocytosed. Endocytosis<sup>37</sup> was classified into phagocytosis and pinocytosis. Phagocytosis was involved the uptake of large particles and is one of the main mechanisms by which particles are taken up by white blood cells. Pinocytosis was a constitutive cell uptake mechanism in most cells. The cationic dendrimers might be taken up into the cells by adsorptive endocytosis through interaction with the negatively charged proteoglycans in the cell membrane.<sup>38,39</sup> However, the neutral dendrimers were presumably endocytosed by non-specific interactions such as hydrophobic and hydrogen bond interactions.<sup>40</sup> As shown by the results in Fig. 5, PEG-*b*-PSD/PAMAM complexes were stable above pH 7.0. The cell uptake of PEG-*b*-PSD/PAMAM complexes followed the mechanisms of neutral dendrimers. The pH value of cytoplasm and lysosomes is around 6.5 and 5.0. All the PEG-*b*-PSD/PAMAM complexes would disintegrate completely in lysosomes after being taken up by tumor cells. Compared with PEG-PAMAM, free PAMAM could destroy the lysosomes more efficiently by the proton pump effect, and release drug faster in the cytoplasm with producing a higher antitumor effect.

**Internalization of PEG-*b*-PSD/PAMAM and LA-PEG-*b*-PSD/PAMAM Complexes** In our study, the pH value of RPMI-1640 medium was 7.4. Figure 11 showed the internalization of PEG-*b*-PSD/PAMAM/DOX complexes and LA-PEG-*b*-PSD/PAMAM/DOX complexes in HepG2 cells. The red stain was DOX fluorescence, and the green stain was the FITC fluorescence in PAMAM. The yellow color on the cells clearly indicates co-localization of green and red. After a 4 h incubation, the cells treated with the LA-PEG-*b*-PSD/PAMAM/DOX complexes showed a clearly higher fluores-

Table 2. The Effect of DOX in Different Formulations on the Growth of H<sub>22</sub> Cells on KM Mice (n=10)

Groups	Number of mice		Body weight (g)		Tumor weight	Inhibition
	Beginning	End	Beginning	End	(g)	(%)
Control	10	10	25.78±1.2	26.81±0.82	1.12±0.28	—
DOX solution	10	10	25.11±1.52	24.38±1.05	0.63±0.18	43.66±15.92*
PAMAM/DOX	10	10	26.34±1.58	25.14±1.98	0.56±0.16	50.36±14.57*
PEG-PAMAM/DOX	10	10	26.51±2.07	26.91±1.33	0.50±0.17	55.56±15.09*
PEG- <i>b</i> -PSD/PAMAM/DOX	10	10	25.92±1.37	26.17±1.28	0.38±0.16	66.07±14.00******
LA-PEG- <i>b</i> -PSD/PAMAM/DOX	10	10	25.88±1.77	26.04±0.79	0.21±0.10	80.87±9.18******

Data were expressed as mean±S.D. \* $p<0.05$ , vs. control group (one-way analysis of variance test); \*\* $p<0.05$ , vs. PEG-*b*-PSD/PAMAM/DOX group; \*\*\* $p<0.05$ , vs. PEG-PAMAM/DOX group; \*\*\*\* $p<0.05$ , vs. PAMAM/DOX group.

cence intensity than PEG-*b*-PSD/PAMAM/DOX complexes, which could be used for qualitatively assessing the degree of PAMAM and DOX taken by the cells. The results of this microscopic cellular uptake study showed that significant targeting ability of PAMAM complexes was obtained by conjugation of lactose with PAMAM.

As shown in Fig. 11A, some cells was stained red only, and this should contribute to the DOX release from the PAMAM in the extracellular domain, allowing uptake by the cells. The results of the drug release study *in vitro* showed that in a short period of time (4 h), the cumulative release of DOX from PAMAM complexes was about 20% at pH 7.4. Figure 11B shows the micrographs of the clearly intense yellow fluorescence in all cells, since large amount of DOX entered the cell with the PAMAM *via* receptor-mediated endocytosis. It is worth noting that HepG2 cells have a relatively large amount of ASGP receptors (150000 binding sites/cell) on their surface that bind and internalize lactose-terminal (asialo-) glycoproteins.<sup>41)</sup> The anti-tumor effect was consistent with the interaction between the lactose moieties of PAMAM complexes and ASGP receptors on HepG2 cells.

**In Vivo Therapeutic Studies** H<sub>22</sub> is a hepatocarcinoma of the mouse and can be used to construct the hepatocyte tumor animal model to evaluate the hepatocyte-targeted delivery mediated by galactose *in vivo*.<sup>42)</sup>

Using H<sub>22</sub> tumor-bearing mice, the anti-tumor efficacy of DOX in different formulations was evaluated. The treatment with LA-PEG-*b*-PSD/PAMAM/DOX complexes inhibited primary tumor growth compared with other control formulations, as shown in Table 2. All of the treatment groups produced a significant anti-tumor effect compared with the physiological saline control group ( $p<0.05$ ), and the relative tumor inhibition produced by the LA-PEG-*b*-PSD/PAMAM/DOX complex group was 80.87%, demonstrating the efficacy of lactose conjugation. In addition, the PEG-*b*-PSD/PAMAM/DOX complex group also produced enhanced tumor regression compared with the PAMAM/DOX group ( $p<0.05$ ), and the PEG-PAMAM/DOX group ( $p<0.05$ ), which might be due to the PEG chain becoming detached from the complexes at the tumor site. In both the *in vitro* and *in vivo* experiments, LA-PEG-*b*-PSD/PAMAM/DOX complexes exhibited better antitumor activity than non-lactose PEG-*b*-PSD/PAMAM/DOX complexes and PEG-PAMAM/DOX. We believe that this drug delivery system may lead to the development of more effective and less toxic liver cancer treatments.

## Conclusion

In this study, we synthesized a pH-sensitive LA-PSD-*b*-

PEG diblock copolymer. pH-sensitive complexes were prepared with PAMAM (G4.0) and LA-PEG-*b*-PSD by electrostatic interaction. The LA-PEG-*b*-PSD/PAMAM complexes can distinguish between a small difference in pH values and exhibit selective targeting and cytotoxicity against HepG2 cells *in vitro*. Finally, the potential to kill tumors *in vivo* was examined in H<sub>22</sub> tumor-bearing mice. We believe this strategy should be generally applicable to the treatment of liver cancers.

**Acknowledgments** This work was supported by a Grant from the National Natural Science Foundation of China (No. 30873181).

## References

- Anil K. P., István J. M., James R. B. J., *Curr. Opin. Chem. Biol.*, **6**, 466—471 (2002).
- Stiriba S. E., Privdoz H. F., Haag R., *Int. Ed. Engl.*, **41**, 1329—1334 (2002).
- Aulenta F., Hayes W., Rannard S., *Eur. Polym. J.*, **39**, 1741—1771 (2003).
- Boas U., Heegaard P. M. H., *Chem. Soc. Rev.*, **33**, 43—63 (2004).
- Svenson S., Tomalia D. A., *Adv. Drug Deliv. Rev.*, **57**, 2106—2129 (2005).
- Durairaj C., Ramakrishna S., Farhan J. A., Roop K. K., Prakash V. D., *Biomaterials*, **28**, 504—512 (2007).
- Bhadra D., Bhadra S., Jain N. K., Jain A., *Int. J. Pharmaceut.*, **257**, 111—124 (2003).
- Kolhe P., Misra E., Kannan R. M., Kannan S., Lieh-Lai M., *Int. J. Pharmaceut.*, **259**, 143—160 (2003).
- Kannan S., Kolhe P., Raykova V., Glibatec M., Kannan R. M., Lieh-Lai M., Bassett D., *J. Biomater. Sci. Polym. Ed.*, **15**, 311—330 (2004).
- Lee E. S., Gao Z. G., Bae Y. H., *J. Controlled Release*, **132**, 164—170 (2008).
- Xu H., Deng Y. H., Chen D. W., Wu H. B., Lu Y., *J. Controlled Release*, **130**, 238—245 (2008).
- Sung W. H., Won H. J., *Polymer*, **49**, 4180—4187 (2008).
- Taluja A., Bae Y. H., *Int. J. Pharmaceut.*, **358**, 50—59 (2008).
- Han S. K., Na K., Bae Y. H., *Colloids Surf. A Physicochem. Eng. Aspects*, **214**, 49—59 (2003).
- Wakebayashi D., Nishiyama N., Yamasaki Y., Itaka K., *J. Controlled Release*, **95**, 653—664 (2004).
- Fallon R. J., Schwartz A. L., *Adv. Drug Deliv. Rev.*, **4**, 49—63 (1989).
- Donati I., Gamini A., Vetere A., Campa C., Paoletti S., *Biomacromolecules*, **3**, 805—812 (2002).
- Wu J., Nantz M. H., Zern M. A., *Front Biosci.*, **7**, 17—25 (2002).
- Chung T. W., Yang J., Akaike T., *et al.*, *Biomaterials*, **23**, 2827—2834 (2002).
- Wu D. Q., Lua B., Chang C., Chen C. S., Wang T., Zhang Y. Y., Cheng S. X., Jiang X. J., Zhang X. Z., Zhuo R. X., *Biomaterials*, **30**, 1363—1371 (2009).
- Kim Y. K., Choi J. Y., Jiang H. L., Arote R., Jere D., Cho M. H., Je Y. H., Cho C. S., *Virology*, **387**, 89—97 (2009).
- Bao F. S., Wei Z., Rong P., Jie H., Ting H., *Colloids Surf. B Biointerfaces*, **70**, 181—186 (2009).
- Feng Z. Q., Chu X., Huang N. P., Wang T., Wang Y., Shi X., Ding Y., Gu Z. Z., *Biomaterials*, **30**, 2753—2763 (2009).



- 24) Muller R. H., Mader K., Gohla S., *J. Pharm. Biopharm.*, **50**, 161—177 (2000).
- 25) Esfand R., Tomalia D. A., *Drug Discov. Today*, **6**, 427—436 (2001).
- 26) Kojima C., Kono M., Maruyama K., Takagishi T., *Bioconjugate Chem.*, **11**, 910—917 (2000).
- 27) D'Emanuele A., Attwood D., *Adv. Drug Deliv. Rev.*, **57**, 2147—2162 (2005).
- 28) Papagiannaros A., Dimas K., Papaioannou G. T., Demetzos C., *Int. J. Pharmaceut.*, **302**, 29—38 (2005).
- 29) Kurtoglu Y. E., Mishra M. K., Kannan S., Kannan R. M., *Int. J. Pharmaceut.*, **384**, 89—194 (2010).
- 30) Park I. K., Park Y. H., Shin B. A., Choi E. S., Kim Y. R., Akaike T., Cho C. S., *J. Controlled Release*, **69**, 97—108 (2000).
- 31) Hashida M., Nishikawa M., Yamashita F., *Adv. Drug Deliv. Rev.*, **52**, 187—196 (2001).
- 32) Gao S. Y., Chen J. N., Xu X. R., Ding Z., Yang Y. H., *Int. J. Pharmaceut.*, **255**, 57—68 (2003).
- 33) Sethuraman V. A., Bae Y. H., *J. Controlled Release*, **118**, 216—224 (2007).
- 34) Holland J. W., Hui C., Cullis P. R., *Biochemistry*, **35**, 2618—2624 (1996).
- 35) Kirpotin D., Hong K., Mullah N., Papahadjopoulos D., Zalipsky S., *FEBS Lett.*, **388**, 115—118 (1996).
- 36) Drummond D. D., Zignani M., Leroux J. C., *Prog. Lipid Res.*, **39**, 409—460 (2000).
- 37) Mukherjee S., Ghosh R. N., Maxfield F. R., *Physiol. Rev.*, **77**, 760—803 (1997).
- 38) Huang M., Ma Z., Khor E., Lim L. Y., *Pharm. Res.*, **19**, 1488—1494 (2002).
- 39) Goncalves C., Mennesson E., Fuchs R., Gorvel J. P., Midoux P., Pichon C., *Mol. Ther.*, **10**, 373—385 (2004).
- 40) Vandamme T. F., Brobeck L., *J. Controlled Release*, **102**, 23—38 (2005).
- 41) Schwartz A. L., Fridovich S. E., Knowles B. B., Lodish H. F., *J. Biol. Chem.*, **256**, 8878—8881 (1981).
- 42) Wang Q., Zhang L., Hu W., Bei Y. Y., Xu J. Y., Wang W. J., Zhang X. N., Zhang Q., *Nanomedicine: Nanotechnology, Biology, and Medicine*, **6**, 371—381 (2010).